



ELSEVIER

Contents lists available at ScienceDirect

MethodsX

journal homepage: www.elsevier.com/locate/mex

Method Article

A detailed manual segmentation procedure for the hypothalamus for 3T T1-weighted MRI



Mohammad Ali^a, Jee Su Suh^b, Milita Ramonas^d, Stefanie Hassel^e, Stephen R. Arnott^f, Stephen C. Strother^f, Luciano Minuzzi^{b,c}, Roberto B. Sassi^g, Raymond W. Lam^g, Roumen Milev^h, Daniel J. Müller^{i,k}, Valerie H. Taylor^e, Sidney H. Kennedy^{j,*}, Benicio N. Frey^{b,c,*}, CAN-BIND Investigator Team

^a Neuroscience Graduate Program, McMaster University, Hamilton, ON, Canada

^b Mood Disorders Program, Department of Psychiatry and Behavioural Neurosciences, McMaster University, Hamilton, ON, Canada

^c Women's Health Concerns Clinic, St. Joseph's Healthcare Hamilton, Hamilton, Ontario, Canada

^d Juravinski Hospital and Cancer Centre, Hamilton Health Sciences, Hamilton, ON, Canada

^e Department of Psychiatry, Cumming School of Medicine, University of Calgary, Calgary, Alberta, Canada

^f Rotman Research Institute, Baycrest, Toronto, ON, Canada

^g Department of Psychiatry, University of British Columbia, Vancouver, BC, Canada

^h Departments of Psychiatry and Psychology, Queen's University, and Providence Care Hospital, Kingston, ON, Canada

ⁱ Department of Psychiatry, University of Toronto, Toronto, ON, Canada

^j Centre for Depression and Suicide Studies, St. Michael's Hospital, Toronto ON, Canada

^k Campbell Family Mental Health Research Institute, Centre for Addiction and Mental Health, Toronto, ON, Canada

ABSTRACT

The hypothalamus is a small grey matter structure which plays a crucial role in many physiological functions. Some studies have found an association between hypothalamic volume and psychopathology, which stresses the need for a standardized method to maximize segmentation accuracy. Here, we provide a detailed step-by-step method outlining the procedures to manually segment the hypothalamus using anatomical T1w images from 3T scanners, which many neuroimaging studies collect as a standard anatomical reference image. We compared volumes generated by manual segmentation and those generated by an automatic algorithm, observing a significant difference between automatically and manually segmented hypothalamus volumes on both sides (left: $U = 222842$, p -value $< 2.2e-16$; right: $U = 218520$, p -value $< 2.2e-16$).

- Significant difference exists between existing automatic segmentation methods and the manual segmentation procedure.
- We discuss potential drift effects, segmentation quality issues, and suggestions on how to mitigate them.

* Corresponding authors.

E-mail address: freymb@mcmaster.ca (B.N. Frey).

- We demonstrate that the present manual segmentation procedure using standard T1-weighted MRI may be significantly more accurate than automatic segmentation outputs.

© 2022 The Author(s). Published by Elsevier B.V.
This is an open access article under the CC BY-NC-ND license
(<http://creativecommons.org/licenses/by-nc-nd/4.0/>)

ARTICLE INFO

Method name: Manual Segmentation of the Hypothalamus using standard 3T anatomical T1w images

Keywords: Hypothalamus segmentation, MRI, Algorithm

Article history: Received 26 July 2022; Accepted 13 September 2022; Available online 17 September 2022

Specifications table

Subject area:	Neuroscience
More specific subject area:	Neuroimaging
Name of your method:	Manual Segmentation of the Hypothalamus using standard 3T anatomical T1w images
Name and reference of original method:	Modified from: Bocchetta, M., Gordon, E., Manning, E., Barnes, J., Cash, D.M., Espak, M., Thomas, D.L., Modat, M., Rossor, M.N., Warren, J.D., Ourselin, S., Frisoni, G.B., Rohrer, J.D. (2015). Detailed volumetric analysis of the hypothalamus in behavioral variant frontotemporal dementia. <i>J Neurol</i> , 262(12), 2635–42. doi: 10.1007/s00415-015-7885-2
Resource availability:	https://surfer.nmr.mgh.harvard.edu/fswiki/HypothalamicSubunits

Introduction

While the hypothalamus accounts for approximately 2% of total brain volume, it has diverse and crucial roles in many physiological functions such as appetite [10], circadian rhythms [3], and the body's stress response system through the hypothalamic-pituitary-adrenal axis [8], among others. As a result, hypothalamic volume has recently been of great interest in various biomedical research areas. Given its role in stress physiology, the extant literature hints at the association between hypothalamus volumetry and neuropsychiatric conditions. For instance, smaller hypothalamic volumes were observed in participants with behavioural variant frontotemporal dementia [2], as well as in individuals with generalized anxiety disorder [11]. In contrast, a recent study observed that subjects with unipolar and bipolar affective disorders had larger hypothalamic volumes [9].

Several studies have been published on how to segment the hypothalamus and its subunits. Bocchetta et al. [2] described how to manually segment the hypothalamus using T1- and T2-weighted MR images, which included a specific segmentation procedure, landmarks, and breakdown of the individual subunits of the hypothalamus. There are also semi-automatic protocols, where human raters set hypothalamic seed voxels, from which the automatic component identifies regions of interest. The algorithm then uses a seed growing technique to analyze surrounding voxels, identifying whether the voxels meet the grey matter probability thresholds for inclusion in the segmentation [12].

Recently, an automatic segmentation algorithm was released and integrated into the FreeSurfer suite with version 7.0. The automatic tool uses data augmentation, which is then used to train a convolutional neural network to segment the hypothalamus and its subunits [1]. Using this procedure, the hypothalamus may be divided into five different compartments, which are delineated slice-by-slice following compartment-specific landmarks.

While these methods are detailed and exhibit good validity, they were designed using high-quality data (i.e., using both T1- and T2- weighted images or high-field imaging) collected for the purpose of fine-grained hypothalamus segmentation. This largely precludes the application of these tools to pre-existing standard 3T anatomical datasets, which may have been collected for volumetric analyses of other cortical and subcortical structures. To fill this gap and aid researchers who may seek to measure hypothalamic volumes in existing T1-weighted datasets, we provide a detailed procedure to manually segment the hypothalamus taking these limitations into account. Using a large 3T dataset originally collected as part of a multi-site clinical trial to identify biomarkers of treatment response in major

depressive disorder (MDD), we further make the case for the need to overcome drift effects associated with manually segmenting large (400+) samples of images to analyze the differences in outcomes between manual and automatic segmentations.

Materials & methods

Image acquisition and participant information

Data were collected as part of a multi-site antidepressant treatment trial in Canada (the Canadian Biomarker Integration Network in Depression; CAN-BIND) [4,5,7]. Each MR image was obtained at 3T using four scanner models across six different sites at baseline (timepoint 1) and 8 weeks post-baseline scan (timepoint 2), following an 8-week open-label trial of escitalopram (10-20mg/day). These scanners included the Discovery MR750 3.0T (GE Healthcare, Little Chalfont, Buckinghamshire, UK), Signa HDxt 3.0T (GE Healthcare, Little Chalfont, Buckinghamshire, UK), TrioTim 3.0T (Siemens Healthcare, Erlangen, Germany), and Intera 3.0T (Philips Healthcare, Best, Netherlands). Each site used a whole-brain turbo gradient echo sequence with the following ranges of parameters: repetition time (TR) = 6.4-1760ms, echo time (TE) = 2.2-3.4s, flip angle = 8-15 degrees, inversion time (TI) = 450-950ms, field of view (FOV) = 220-256mm, acquisition matrix = 256 × 256 – 512 × 512, 176-192 contiguous slices at 1mm thickness with voxel dimensions of 1mm³ isotropic. The total acquisition time of each image ranged between 3:30 min to 9:50 min. Upon each scan, the raw data was visually inspected to determine if there were any artifacts that would compromise the quality of the image for further processing. If it was determined the image could not be used, a re-scan of the participant was initiated, if time permitted.

Participant inclusion/exclusion criteria

Table 1 summarizes the inclusion and exclusion criteria for recruitment of MDD participants. Participants with no psychiatric or unstable medical conditions between the ages of 18-60 with sufficient fluency in English to complete study procedures were also included as healthy control subjects. They were matched to MDD participants by age and sex [5].

Blinding procedure

Each image file was stripped of multiple identifier tags, which included timepoint and site. Two independent raters (MA, JSS) remained blind to diagnostic group. Each rater underwent a 'training period' where they segmented over 100 images that were not included in the final data collection. To quantify possible drift effects remaining after this training period, both raters manually segmented the entire dataset twice with a six-month test-retest interval between the segmentations.

Hardware

All segmentations were conducted on a 27-inch (2560 × 1440) 2013 iMac using a standard mouse for tracing. The graphics card within the iMac was a NVIDIA GeForce GT 755M 1 GB.

Hypothalamus anatomy

The hypothalamus is a small gray matter structure that is situated directly above the pituitary gland and below the thalamus. Anteriorly, the hypothalamus is bounded by the lamina terminalis and the anterior commissure. Posteriorly, it has boundaries along the midbrain and mammillary bodies. In the coronal view, the walls of the hypothalamus can be divided into four different surfaces: superior, inferior, lateral, and medial. Superior to the wall of the hypothalamus is the thalamus, separated by the hypothalamic sulcus. Inferiorly, it is bounded by the walls of the third ventricle. The lateral surfaces shares boundaries with the internal capsule, thalamus, and subthalamus. Lastly, the medial surface stretches to the walls of the third ventricle [6].

Table 1

Inclusion/Exclusion criteria of study participants

Inclusion and exclusion criteria for participants	
<i>Inclusion Criteria</i>	<ul style="list-style-type: none"> • Participants: 18 to 60 years of age • DSM-IV-TR criteria for MDE in MDD, as confirmed by the MINI • Depressive episode duration ≥ 3 months • No psychotropic medications use for at least 5 half-lives (i.e., 1 week for most antidepressants, 5 weeks for fluoxetine) before baseline • MADRS Score ≥ 24 • Sufficient fluency in English to complete the interviews and self-report questionnaires
<i>Exclusion Criteria</i>	<ul style="list-style-type: none"> • Bipolar I or Bipolar II disorder diagnosis • Any other psychiatric diagnosis considered as the primary diagnosis • Any major personality disorder diagnosis (e.g., antisocial, borderline), which may potentially interfere with participation defined by clinician • High suicidal risk, determined by clinician judgment • History of substance dependence/abuse within the past 6 months • Significant neurological disorders, head trauma, or other unstable medical conditions • Psychosis in the current episode • Pregnant or breastfeeding • Contraindications of MRI • High risk for hypomanic switch (i.e., history of antidepressant-induced hypomania). • Failed 4 or more adequate pharmacologic interventions determined by the ATHF • Previously failed or showed intolerance to aripiprazole or escitalopram • Began psychological treatment within the past 3 months with the intent of continuing treatment

DSM-IV-TR, Diagnostic and Statistical Manual of Mental Disorders, Fourth Edition, Text Revision; MDE, Major Depressive Episode; MDD, Major Depressive Disorder; MINI, Mini International Neuropsychiatric Interview; MADRS, Montgomery-Åsberg Depression Rating Scale; ATHF, Antidepressant Treatment History Form (Adapted from Table 1 of [5])

Manual segmentation of the hypothalamus

The hypothalamus was manually segmented by the two independent raters using an open-source software called ITK-SNAP version 3.8.0, chosen for its user-friendly segmentation tools. The brush tool was used at its smallest size (1mm, isotropic) to trace and segment the hypothalamus.

To compensate for the absence of T2-weighted images for additional contrast, we generated gray matter tissue probability maps (GM-TPMs) for each MR image using the VBM Segment tool available in SPM 12 in Matlab (Wolff et al., 2013). We superimposed the GM-TPM at an opacity level of 8% over the T1-weighted image to assist with differentiating between grey and white matter in determining the outer boundaries of the hypothalamus. The boundaries illustrated by Bocchetta et al., [2] served as a guideline to manually segment the hypothalamus with slight variations (Figure 1). See Table 2

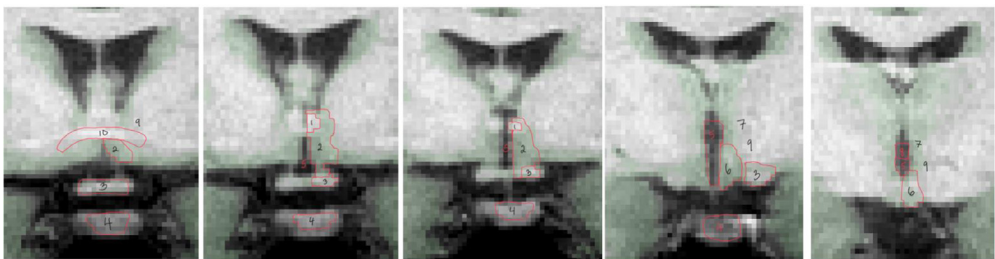






Fig. 1. Diagram of the surrounding area of the hypothalamus




Table 2

Stepwise summary of the manual segmentation method

Step	Directions	Example segmentation
1.	Open raw image and magnify the image to 11 px/mm. Set paint brush size to 1, check 'isotropic'.	
2.	Apply GM-TPM and work in coronal view, with the sagittal and horizontal planes of view visible for reference. To apply GM-TPM, open image layer inspector, which is found in the main toolbar. Select the specific GM-TPM by opening the desired file and add as a semi-transparent overlay. Then select "black to green" as overlay colour. To adjust contrast of GM-TPM, return to image layer inspector and select the contrast option and adjust contrast to ~8%.	
3.	Identify anterior commissure, which is seen as a white band under the third ventricle and directly above the hypothalamus (outlined in black). Begin segmentation here.	
4.	Continue segmenting in the rostral to caudal direction using the edges of the optic tract as a horizontal boundary for the hypothalamus. Initially exclude the fornix, which is seen as the two white bulbs (outlined in black) attached to the third ventricle by segmenting around it as it first appears.	

(continued on next page)

Table 2 (continued)

Step	Directions	Example segmentation
5	As the fornix descends into the body of the hypothalamus, include it in the segmentation.	
6	Include the mammillary bodies in the segmentation.	
7	Once the mammillary bodies disappear, end segmentation.	

1=Fornix, 2=Hypothalamus, 3=Optic Tract, 4=Pituitary Gland, 5=Third Ventricle, 6=Mamillary Bodies, 7=Thalamus, 8=Hypothalamus Sulcus, 9=Internal Capsule, 10=Anterior Commissure

for a detailed sequence of manual segmentation steps and [Figure 2](#) for a slice-by-slice representation of a full volume segmentation. Although Bocchetta et al. [2] excluded the fornix entirely, we included it in the segmentation starting from the slice where the medial edge of the fornix begins to move away from the third ventricle, moving in the rostral-caudal direction. This was necessary due to the difficulty and additional variation that would be associated with visually discerning the boundaries of the fornix as it begins to travel further into the GM caudally.

We segmented the hypothalamus moving in the rostral to caudal direction in the coronal view while using the horizontal and sagittal views for cross reference. The coronal view was most often used as it offered easier identification of the hypothalamus and its surrounding boundaries. We also alternated between segmenting the left and right hemispheres first with each subsequent image, reducing the visibility of the first segmentation to 0 once it was completed, thus minimizing any visual bias that may occur. We began the segmentation once the anterior commissure became completely visible, ending with the disappearance of the mammillary bodies. As a result, the whole

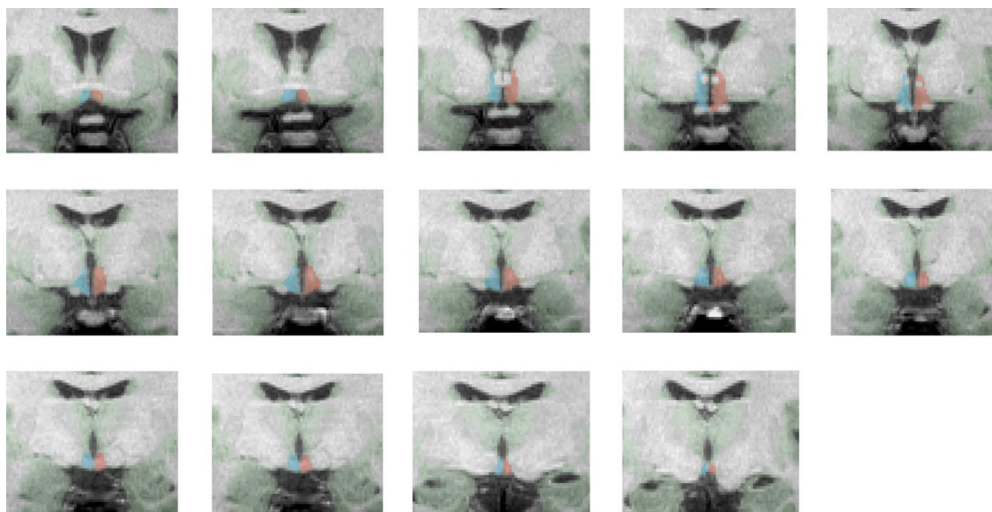


Fig. 2. Schematic of a full manual hypothalamic segmentation. Blue = Right Hypothalamus; Red = Left Hypothalamus

volume of the hypothalamus comprised the three main regions of the hypothalamus, including the preoptic region, anterior hypothalamic region, and the mammillary bodies.

Automatic segmentation of the hypothalamus

The same images underwent automatic segmentation using the tools developed by Billot et al. [1] included with the FreeSurfer version 7.0 release. The pipeline is publicly available and guidelines can be found at <https://surfer.nmr.mgh.harvard.edu/fswiki/HypothalamicSubunits>. The automatic pipeline divides the hypothalamus into five different subunits for the left and right side of the hypothalamus, which are the anterior-inferior, anterior-superior, posterior, inferior tubular, and superior tubular subunits. This algorithm excludes the fornix from all sections of the volume. Total volume for the hypothalamus was calculated by adding the volumes of each of the subunits for the left and right sides.

Statistical analyses

All statistical analyses were conducted in R version 1.3.1093. To measure the inter-rater reliability of the segmentations produced by the two independent raters, intra-class coefficients (ICC) were calculated for left, right, and total hypothalamic volume values produced by each rater. Specifically, the ICC model [3,1] (Shrout and Fleiss convention) was used as each subject was assessed by the two raters of interest. Segmentation values that exhibited a difference of two standard deviations (SD) or more between the two raters were independently segmented again (Nogovitsyn et al., 2019). Intra-rater agreement scores were calculated using 50 randomly chosen images that were segmented twice by both raters. Dice scores were also calculated by overlaying the manual segmentations created by the individual raters and then determining the percentage of overlap between the segmentations.

Paired t-tests were conducted to determine any volume changes in healthy participants from baseline to 8 weeks. This was done to evaluate whether any additional factors, such as image quality or errors in manual segmentation, may have affected volumetric estimates.

A paired t-test was conducted between manually segmented hypothalamus volumes of the entire dataset repeated at two timepoints to determine the magnitude of a potential drift effect across time, observed as a slight change in test-retest manual segmentation volumes. In addition, the Mann-Whitney U test was conducted to determine if significant differences existed between volume

Table 3
Final ICC and Dice values

	Manual Segmentation (between raters)		Automatic vs Manual Segmentation		
	Final ICC	Final Dice	Final ICC	ICC (Fornix Removed)	Final Dice
Left	0.85	0.84	0.34	0.31	0.71
Right	0.83	0.82	0.43	0.37	0.71
Left+Right	0.80	0.83	0.41	0.29	0.71

measures generated using the automatic hypothalamus segmentation algorithm [1] and our manual hypothalamus segmentation procedure.

Lastly, ICC scores, the Mann-Whitney U test, and Dice scores were also calculated between the set of manual segmentations with the fornix removed throughout all the slices and the automatic segmentations, to obtain the most accurate estimate of spatial overlap between the methods.

Expert check

To ensure accuracy and assess quality, a certified neuroradiologist (MR) was provided with 15% of the manual segmentations from each site to provide an expert opinion on the accuracy of the hypothalamic segmentation, for a total of 50 images. Each segmentation was rated on accuracy according to visible landmarks by a numerical rating (1-3), where a 1 signified a need to re-segment the entire image, a 2 indicated only minor edits, and a 3 identified that no further changes needed to be made. This expert opinion check served to review and flag whether systematic errors occurred in our manual segmentations. In addition to assessing the quality of manually segmented images, the neuroradiologist was also provided with 15% of the automatically segmented images to assess quality and accuracy. The same rating scale was used for the automatically segmented images.

Method validation

Manual segmentation analysis

The ICC values for the initial round of manual hypothalamus segmentation by two independent raters prior to additional rounds of segmentations were in the range of 0.63-0.64 for left, right and total volumes. After screening for volume discrepancies >2 SD, final ICC values between the two independent raters ranged between 0.8-0.85 for left, right, and total volumes. Final Dice scores were also within the range of 0.79-0.8 (Table 3).

Paired t-tests revealed no significant differences in hypothalamic volumes amongst healthy comparison participants from baseline to week 8 (left: $t = 0.18789$, $p\text{-value} = 0.8515$; right: $t = 0.058671$, $p\text{-value} = 0.9534$).

Paired t-tests revealed a significant effect of time on mean volumes segmented twice, indicating a drift effect occurred following a 6-month test-retest interval (Figure 3; left: $t = -9.8142$, $p\text{-value} < 2.2e-16$; right: $t = -4.2192$, $p\text{-value} = 2.938e-05$).

Comparison between manual segmentation and automatic segmentation

A Mann-Whitney U-test revealed significant differences between mean hypothalamus volume values generated by the automatic and manual methods (left: $U = 222842$, $p\text{-value} < 2.2e-16$; right: $U = 218520$, $p\text{-value} < 2.2e-16$; Table 4). Figure 4 illustrates the extent of spatial overlap between representative manual and automatic hypothalamus segmentations. The difference remained significant even after the fornix was removed from the manual segmentations (left: $U = 223145$, $p\text{-value} < 2.2e-16$; right: $U = 219062$, $p\text{-value} < 2.2e-16$).

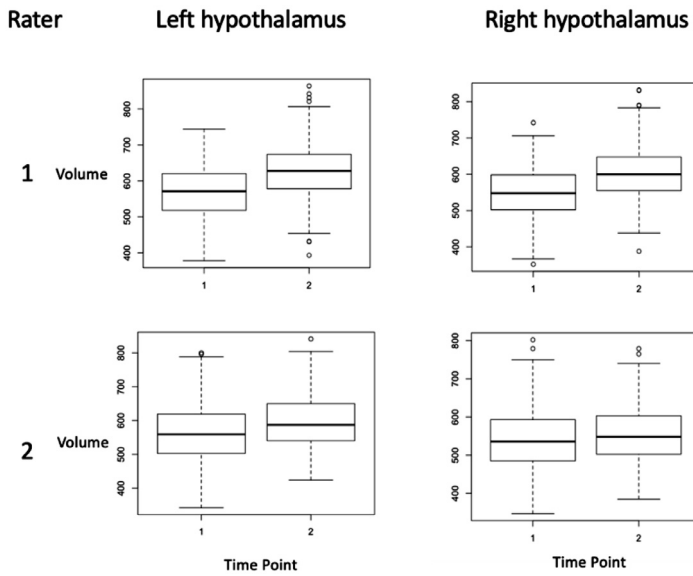


Fig. 3. Drift effects of manual segmentations performed at timepoints 1 and 2 (6-month test-retest interval)

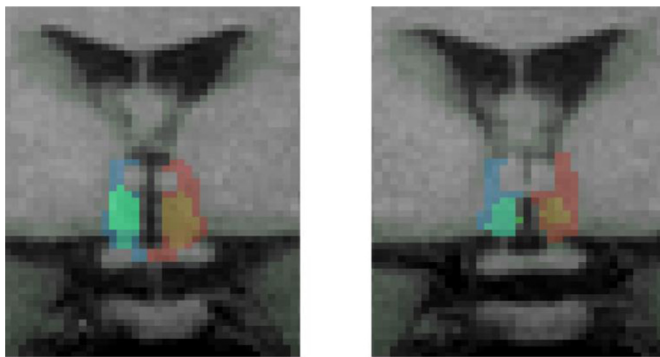


Fig. 4. Visual illustration of superimposed automatic and manual segmentation. Blue/red = manual segmentation; turquoise/brown= automatic segmentation

Table 4

Comparison between automatic vs manual hypothalamus segmentation within all sites used for analysis. TGH = Toronto General Hospital; UCA = University of Calgary; CAM = Centre for Addiction and Mental Health; MCU = McMaster University; UBC = University of British Columbia; QNS = Queen’s University

	All Sites U	p-value	TGH p-value	UCA p-value	CAM p-value	MCU p-value	UBC p-value	QNS p-value
Left	222842	2.2e-16	*	*	*	*	*	*
Right	218520	2.2e-16	*	*	*	*	*	*
Left + Right	222191	2.2e-16	*	*	*	*	*	*

* p-value < 0.0001

Expert check

No systematic errors were detected by the expert reviewer for manually segmented images. Minor changes were suggested such as the removal of a slice near the end of the segmentation, where the mamillary bodies begin to disappear. Additionally, the automatic pipeline required adjustments, such as the addition of slices in the beginning of the segmentation when the corpus callosum first appeared and removal of a slice as the mamillary bodies begin to disappear.

Discussion

In this paper, we provide a practical guide on manual segmentation of the hypothalamus in 3T T1-weighted images, contrasting the results with those generated by an automatic algorithm. A significant difference between volumes generated by manual and automatic segmentation was observed. Furthermore, the heterogeneity of hypothalamic structure between participants may decrease the accuracy of automatic methods, whereas manual segmentation allows the rater to assess varying boundaries intuitively and with greater flexibility. In addition, other structures such as the third ventricle and optic tract can vary significantly between individuals, which can affect the upper and horizontal boundaries of the hypothalamus. Lastly, visual inspection of images suggested that image quality can vary between scanners in a multi-site study, which can potentially affect the delineation of boundaries. Therefore, we recommend that if automatic segmentation is used, manual inspection and adjustments of each segmentation should be made to ensure accuracy, but that manual segmentation remains the gold standard when measuring hypothalamic volumes.

Nevertheless, there are certain limitations to manual segmentation, one of which includes a drift effect when comparing manual segmentations performed twice across a 6-month interval. To mitigate this, we recommend segmenting a minimum of 100 images for training purposes prior to manual segmentation for analysis. It is likely that over a period of time, raters are simply improving at manual segmentation with repeated practice. This may confound certain statistical analyses, particularly with respect to longitudinal analyses if images are being segmented in timepoint order. Additionally, manually segmenting large amounts of images may cause fatigue that might also affect segmentation quality. Standardizing the number of segmentations to a set number of images per day (e.g., 15-20) will aid in mitigating fatigue, reducing human error, and increasing consistency. Our own range of 15-20 images per day was determined from our experience of segmenting large numbers of images on a day-to-day basis.

Despite the above limitations, the method we describe here has significant advantages over existing methods. First, it provides a manual segmentation guide applicable to any standard 3T T1-weighted anatomical dataset in the absence of T2-weighted images. This would allow for the analysis of this structure in pre-existing datasets originally collected for general whole-brain morphometric analyses. Second, we present a standardized, step-by-step guide to segmentation using an open-source, user-friendly software; pre-existing expertise in programming languages or complex medical image analysis software is not required. We hope this will encourage more work in this area across a variety of conditions/disorders. Third, we incorporated expert opinion by a professional neuroradiologist to confirm that there were no systematic errors being made in our segmentations. We suggested a framework a professional neuroradiologist could use to systematically quality check manual segmentations. Lastly, if an automatic pipeline is used, our schematics can serve as a guide to manually inspect the outputs.

Conclusion

In this study, we provide a detailed method to manually segment the hypothalamus to reduce the technical barriers without sacrificing data quality. While innovative techniques to automatically segment the hypothalamus are in active development, we describe a manual segmentation procedure that provides an accurate analysis of volume and should remain the gold standard until automatic segmentation algorithms increase in accuracy and flexibility in standard 3T T1-weighted images that are most commonly collected in clinical research.

Ethics statements

All participants consented to the use of their data after being provided with detailed information regarding the study, data collection, and use.

Declaration of competing interest

Dr. Milev has received research grants from CAN-BIND, CIHR, Janssen, Lallemand, Lundbeck, Nubiyota, OBI and OMHF. Additionally, Dr. Milev has received speaking and consulting honoraria from AbbVie, Allergan, Janssen, KYE, Lundbeck, Otsuka, and Sunovion. Dr. Lam has received honoraria or research funds from Allergan, Asia-Pacific Economic Cooperation, BC Leading Edge Foundation, CIHR, CANMAT, Canadian Psychiatric Association, Hansoh, Healthy Minds Canada, Janssen, Lundbeck, Lundbeck Institute, Michael Smith Foundation for Health Research, MITACS, Ontario Brain Institute, Otsuka, Pfizer, St. Jude Medical, University Health Network Foundation, and VGH-UBCH Foundation. Dr. Strother is the Chief Scientific Officer of ADMdx, Inc., which receives NIH funding, and currently has research grants from Brain Canada, CIHR, the Ontario Brain Institute in Canada. Dr. Kennedy has received research funding or honoraria from the following sources: Abbott, Alkermes, Allergan, BMS, Brain Canada, Canadian Institutes for Health Research (CIHR), Janssen, Lundbeck, Lundbeck Institute, Ontario Brain Institute, Ontario Research Fund (ORF), Otsuka, Pfizer, Servier, Sunovion and Xian-Janssen.

All other authors have no conflict of interest.

Data Availability

Data will be made available on request.

CRediT authorship contribution statement

Mohammad Ali: Conceptualization, Methodology, Writing – original draft. **Jee Su Suh:** Conceptualization, Methodology, Writing – original draft. **Milita Ramonas:** Validation, Writing – review & editing. **Stefanie Hassel:** Investigation, Writing – review & editing. **Stephen R. Arnott:** Investigation, Writing – review & editing. **Stephen C. Strother:** Investigation, Resources, Writing – review & editing. **Luciano Minuzzi:** Writing – review & editing. **Roberto B. Sassi:** Writing – review & editing. **Raymond W. Lam:** Investigation, Resources, Writing – review & editing. **Roumen Milev:** Investigation, Resources, Writing – review & editing. **Daniel J. Müller:** Investigation, Resources, Writing – review & editing. **Valerie H. Taylor:** Investigation, Resources, Writing – review & editing. **Sidney H. Kennedy:** Investigation, Resources, Funding acquisition, Writing – review & editing. **Benicio N. Frey:** Investigation, Resources, Supervision, Writing – review & editing.

Acknowledgments

Funding: This study was supported partially by the Ontario Ministry of Research and Innovation (Early Research Award – Dr. Frey). The platform for neuroimaging was supported partially by a CIHR grant (Co-PIs: Drs. Kennedy and MacQueen, MOP 125880). The Canadian Biomarker Integration Network in Depression is an Integrated Discovery Program partnered with and financially supported from the Ontario Brain Institute, which is an independent non-profit corporation, which is partially funded by the Ontario government. The opinions, results, and conclusions are those of the authors and no endorsement by the Ontario Brain Institute is intended or should be inferred. Additional funding was provided by CIHR, Lundbeck, Bristol-Myers Squibb, Pfizer, and Servier. Funding and/or in-kind support is additionally provided by the investigators' universities and academic institutions. All study medications were independently purchased at wholesale market values.

References

- [1] B. Billot, M. Bocchetta, E. Todd, A.V. Dalca, J.D. Rohrer, J.E. Iglesias, Automated segmentation of the hypothalamus and associated subunits in brain MRI, *Neuroimage* 223 (117287) (2020), doi:[10.1016/j.neuroimage.2020.117287](https://doi.org/10.1016/j.neuroimage.2020.117287).
- [2] M. Bocchetta, E. Gordon, E. Manning, J. Barnes, D.M. Cash, M. Espak, D.L. Thomas, M. Modat, M.N. Rossor, J.D. Warren, S. Ourselin, G.B. Frisoni, J.D. Rohrer, Detailed volumetric analysis of the hypothalamus in behavioral variant frontotemporal dementia, *J. Neurol.* 262 (12) (2015) 2635–2642, doi:[10.1007/s00415-015-7885-2](https://doi.org/10.1007/s00415-015-7885-2).
- [3] I. Heuser, M. Deuschle, A. Weber, A. Kniest, C. Ziegler, B. Weber, M. Colla, The role of mineralocorticoid receptors in the circadian activity of the human hypothalamus- pituitary-adrenal system: effect of age, *Neurobiol. Aging* 21 (4) (2000) 585–589 PMID: 10924776, doi:[10.1016/s0197-4580\(00\)00145-7](https://doi.org/10.1016/s0197-4580(00)00145-7).
- [4] S.H. Kennedy, R.W. Lam, S. Rotzinger, R.V. Milev, P. Blier, J. Downar, K.R. Evans, F. Farzan, J.A. Foster, B.N. Frey, P. Giacobbe, G.B. Hall, K.L. Harkness, S. Hassel, Z. Ismail, F. Leri, S. McInerney, G.M. MacQueen, L. Minuzzi, D.J. Müller, S.V. Parikh, F.M. Placenza, L.C. Quilty, A.V. Ravindran, R.B. Sassi, C.N. Soares, S.C. Strother, G. Turecki, A.L. Vaccarino, F. Vila-Rodriguez, J. Yu, R. Uher, CAN-BIND Investigator Team, Symptomatic and functional outcomes and early prediction of response to escitalopram monotherapy and sequential adjunctive aripiprazole therapy in patients with major depressive disorder: A CAN-BIND-1 Report, *J. Clin. Psychiatry* 80 (2) (2019) 18m12202 PMID: 30840787, doi:[10.4088/JCP.18m12202](https://doi.org/10.4088/JCP.18m12202).
- [5] R.W. Lam, R. Milev, S. Rotzinger, A.C. Andreazza, P. Blier, C. Brenner, Z.J. Daskalakis, M. Dharsee, J. Downar, K.R. Evans, F. Farzan, J.A. Foster, B.N. Frey, J. Geraci, P. Giacobbe, H.E. Feilolter, G.B. Hall, K.L. Harkness, S. Hassel, Z. Ismail, F. Leri, M. Liotti, G.M. MacQueen, M.P. McAndrews, L. Minuzzi, D.J. Müller, S.V. Parikh, F.M. Placenza, L.C. Quilty, A.V. Ravindran, T.V. Salomon, C.N. Soares, S.C. Strother, G. Turecki, A.L. Vaccarino, F. Vila-Rodriguez, S.H. Kennedy, CAN-BIND Investigator Team, Discovering biomarkers for antidepressant response: protocol from the Canadian biomarker integration network in depression (CAN-BIND) and clinical characteristics of the first patient cohort, *BMC Psychiatry* 16 (105) (2016) PMID: 27084692; PMCID: PMC4833905, doi:[10.1186/s12888-016-0785-x](https://doi.org/10.1186/s12888-016-0785-x).
- [6] R.M. Lechan, R. Toni, et al., Functional anatomy of the hypothalamus and pituitary, in: KR Feingold, B Anawalt, A Boyce, et al. (Eds.), *Endotext* [Internet] editors, MDText.com, Inc.; 2000-, South Dartmouth (MA), 2016 Available from: <https://www.ncbi.nlm.nih.gov/books/NBK279126/>.
- [7] G.M. MacQueen, S. Hassel, S.R. Arnott, A. Jean, C.R. Bowie, S.L. Bray, A.D. Davis, J. Downar, J.A. Foster, B.N. Frey, B.I. Goldstein, G.B. Hall, K.L. Harkness, J. Harris, R.W. Lam, C. Lebel, R. Milev, D.J. Müller, S.V. Parikh, S. Rizvi, S. Rotzinger, G.B. Sharma, C.N. Soares, G. Turecki, F. Vila-Rodriguez, J. Yu, M. Zamyadi, S.C. Strother, S.H. Kennedy, CAN-BIND Investigator Team, The Canadian Biomarker Integration Network in Depression (CAN-BIND): magnetic resonance imaging protocols, *J. Psychiatry Neurosci.* 44 (4) (2019) 223–236 PMID: 30840428; PMCID: PMC6606427, doi:[10.1503/jpn.180036](https://doi.org/10.1503/jpn.180036).
- [8] M.G. Oyola, R.J. Handa, Hypothalamic-pituitary-adrenal and hypothalamic-pituitary- gonadal axes: sex differences in regulation of stress responsivity, *Stress* 20 (5) (2017) 476–494 Epub 2017 Aug 31. PMID: 28859530; PMCID: PMC5815295, doi:[10.1080/10253890.2017.1369523](https://doi.org/10.1080/10253890.2017.1369523).
- [9] S. Schindler, L. Schmidt, M. Stroske, M. Storch, A. Anwander, R. Trampel, M. Straub, U. Hegerl, S. Geyer, P. Schönknecht, Hypothalamus enlargement in mood disorders, *Acta Psychiatr. Scand.* 139 (1) (2019) 56–67, doi:[10.1111/acps.12958](https://doi.org/10.1111/acps.12958).
- [10] K. Suzuki, K.A. Simpson, J.S. Minnion, J.C. Shillito, S.R. Bloom, The role of gut hormones and the hypothalamus in appetite regulation, *Endocr. J.* 57 (5) (2010) 359–372 Epub 2010 Apr 14. PMID: 20424341, doi:[10.1507/endocrj.k10e-077](https://doi.org/10.1507/endocrj.k10e-077).
- [11] R. Terlevic, M. Isola, M. Ragogna, M. Meduri, F. Canalaz, L. Perini, G. Rambaldelli, L. Travan, E. Crivellato, S. Tognin, G. Como, C. Zuiani, M. Bazzocchi, M. Balestrieri, P. Brambilla, Decreased hypothalamus volumes in generalized anxiety disorder but not in panic disorder, *J. Affect. Disord.* 146 (3) (2013) 390–394 Epub 2012 Oct 18. PMID: 23084182, doi:[10.1016/j.jad.2012.09.024](https://doi.org/10.1016/j.jad.2012.09.024).
- [12] J. Wolff, S. Schindler, C. Lucas, A.S. Binninger, L. Weinrich, J. Schreiber, U. Hegerl, et al., A semi-automated algorithm for hypothalamus volumetry in 3 tesla magnetic resonance images, *Psychiatry Res.: Neuroimaging* 277 (July) (2018) 45–51, doi:[10.1016/j.pscychresns.2018.04.007](https://doi.org/10.1016/j.pscychresns.2018.04.007).